

---

# Modelling the relationship between the brain's structural and functional connectome

---

An Xuelong, Chen Tianchi, Cheng Zijie, Dziojeva Luba, Fuchs Naomi, Henine Ahmed

## Abstract

"The core principle of Hebbian learning is that neurons that fire together, wire together". We perform exploratory analysis of the brain's structural and functional connectome by computing metrics over an undirected graph representation of them, yielding insight into clustering, communication efficiency, connectivity and distance paths amongst cortical brain regions. We next build linear models of varying complexity and assumptions to explore whether the functional connectome can be predicted from the structural connectome. We find that the reconstruction of graph networks is insightful but challenging because it's highly dependent on a-priori assumptions on graph structure. We also find that functional connectivity can be captured between regions that are structurally, directly and indirectly, connected.

## 1. Introduction and motivation

The study of brain organization, which we now refer to as **connectome** both in the functional and structural domain, has overarching scientific and clinical implications. It remains an open challenge to accurately model the highly heterogeneous interaction between the brain's structure and associated functions. Despite its difficulty, the thorough understanding of brain's structural and functional connectivity can serve as biomarkers of brain states like high-level cognition, or monitor brain pathologies such as Alzheimer. Thus, it altogether makes **connectomics** a worthy endeavor to pursue by the scientific community (Deligianni et al., 2013).

Thanks to the widespread adoption of brain mapping techniques such as magnetic resonance imaging (MRI), vast quantities of data measuring anatomical or functional connection patterns are available (Rubinov & Sporns, 2010). Diffusion MRI (dMRI) (Figure 1) measures the random motion of water molecules, which can be harnessed to infer the distribution of one or more axonal bundle orientations, and as such reconstruct white matter pathways. Resting-state MRI (rs-MRI) (Figure 2) measures sequences of blood oxygen level-dependent (BOLD) signal (delivery of blood to active neuronal tissue) of a patient at rest. This serves as a proxy for brain activity, whereby a functional time series is obtained at each voxel location and connectivity

is inferred from the correlation between these time-series (Wu et al., 2021).

In tandem with advances in machine learning (ML) tools, connectomics enjoy an unprecedented opportunity to analyze and gain insights from this multimodal data. One such approach is to abstract the brain MRI data as a complex network: a graph  $\mathcal{G} = (\mathcal{V}, \mathcal{E})$  where nodes  $\mathcal{V}$  correspond to brain regions connected by edges  $\mathcal{E}$  representing anatomical tracts or functional associations. Such graph is undirected because neither dMRI nor rs-fMRI tell us about the direction of information flow. The elements of the matrix may either be binary indicating the presence or absence of a connection, or continuous indicating the 'strength' of the connection. From such abstraction, we can employ graph theory (see Pavlopoulos et al. (2011)) for its analysis to gain insight on properties that translate into understanding of the brain's organization.

In this work, we first explore how computing different graph metrics like mean shortest path shed insight into the brain's connectome, and explore the effect of certain parameters on these graph-theoretical properties, as planned in Section 2.1. We next build 8 linear models to study the relationship between functional connection weights and structural connection weights, subject to different experimental settings/assumptions, as laid out in Section 2.2.

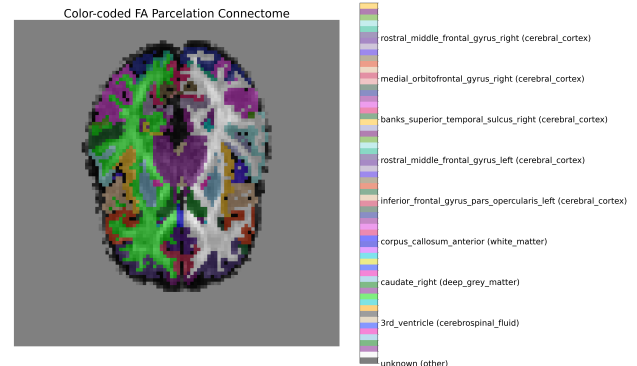


Figure 1. Illustration of a fractional anisotropy (FA) map of a parcelated brain region at slice 30 for a patient

## 2. Methodology

For the first half of our work, we collect the structural and functional MRI for a single patient. We obtain their fractional anisotropy map  $\mathcal{D} \in \mathbb{R}_+^{V \times V \times S}$ , where  $V = 96$  is

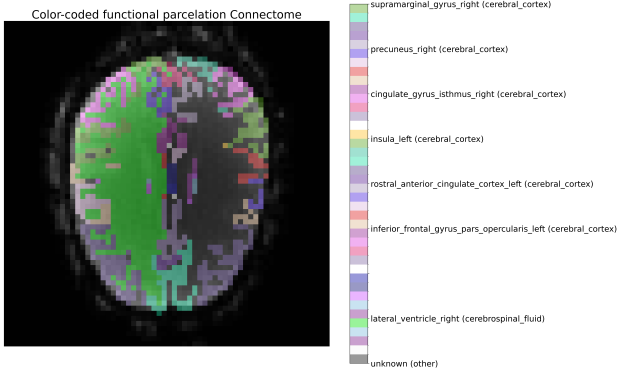


Figure 2. Illustration of the rs-MRI of a parcelated brain region at slice 15, and timestep 12 for a patient

number of voxels, and  $S = 60$  is number of slices. We also collect their rs-MRI data  $\mathcal{R} \in \mathbb{R}^{V \times V \times S \times T}$ , where  $T$  is amount of timesteps, and  $V = 64, S = 30, T = 15$ .

## 2.1. Graph metrics

We manually threshold  $\mathcal{D}$  at different values between 0.1 and 0.8 at steps of 0.1, setting subthreshold voxels to zero, yielding sparser maps as the threshold increases. Voxels mostly disappear in the middle of the brain, while the ones on the surrounding area remain because they have higher white matter integrity. We collect corresponding undirected, binary  $\mathcal{G}$  representations at each threshold, where  $|\mathcal{V}| = 68$  cortical regions. At the functional space, we extract an average time series in each cortical region from  $\mathcal{R}$ , and then derive a correlation matrix following a shrinkage approach by Schäfer & Strimmer (2005). Such correlation matrix have negative values which are conceptually *inhibiting* connections where increased activity in a region is associated with decreased activity in the other. We vary its shrinkage parameter *lambda* between 0.1 and 0.8 at steps of 0.1, yielding sparser resulting matrices. We binarize the matrix at each threshold with a correlation value of 0.1.

Using the brain connectivity toolbox (BCT), for the binarized, undirected graph  $\mathcal{G}$  representations of  $\mathcal{D}$  and  $\mathcal{R}$ , we compute the following metrics with a brief explanation (see Farahani et al. (2019) for more details):

1. **Mean shortest path (MSP):** average distance between any two nodes in  $\mathcal{G}$ , which sheds insights into the efficiency of communication between cortical regions. We ignore nonexistent paths between a pair of nodes.
2. **Global efficiency (GE):** inverse of the mean shortest path between all pairs of nodes in a network. It quantifies the efficiency of information transfer across the entire network.
3. **Mean clustering coefficient (MCC):** average number of connections between neighboring nodes. It quantifies the degree of clustering or cliquishness within the

network.

4. **Edge density (ED):** proportion of existing edges in a network relative to the total possible edges. It quantifies the overall level of connectivity within the network

These graph metrics provide theoretical insights of the brain’s organizational principles. For instance, the average clustering coefficient reflects the presence of tightly knit groups of regions, indicative of specialized processing. Furthermore, by computing these metrics, researchers can identify differences in brain organization across individuals, serving as biomarkers between healthy and diseased states.

## 2.2. Linear models

For the second half of our work, we collect the structural  $\mathcal{S} \in \mathbb{R}_+^{N \times V \times V}$  and functional correlation matrices  $\mathcal{F} \in \mathbb{R}^{N \times V \times V^1}$  for  $N = 19$  patients. We propose 8 linear regression (LR) models predicting the functional from the structural connectome, detailed in Table 1. We account for direct connections, as well as one-hop, indirect ones computed using Algorithm 1. This can reveal how functional interactions are supported by the underlying anatomical pathways, providing insights into phenomena like brain plasticity. We benchmark these linear models under 6 experimental settings, wherein each setting, for each model, we evaluate the Akaike and Bayesian information criteria (AIC and BIC), and perform leave-one-out (LOO) cross-validation (CV) to evaluate its predictive value in terms of the mean square error (MSE):

1. **Edge-wise fitting:** Following Table 1, we treat each entry in  $\mathcal{S}$  and  $\mathcal{F}$  as a datapoint and fit a LR coefficient for each. Each LR coefficient for each model is estimated through ordinary least squares (OLS) using gradient descent, i.e., by minimizing  $\theta_{ij}^* = \arg \min \theta_{ij} \sum_{i,j} (f_{ij}, m_\theta(x_{ij})) + p(\theta_{ij})$ , where the parameter(s)  $\theta_{ij} \subseteq [\alpha_{ij}, \beta_{ij}, \gamma_{ij}, \delta_{ij}]$  and input feature(s)  $x_{ij}$  vary depending on the model architecture,  $f_{ij}$  is each functional connection,  $m_\theta$  is the model, and  $p(\theta)$  is a *penalization* term, where for LR it’s equal to 0.
2. **Edge-wise fitting with Lasso:** The same as the first setting, but penalizing each LR coefficient using L1-regularization (Deligianni et al., 2013), i.e.,  $p(\theta_{ij}) = \lambda_{ij} \sum_{i,j} |\theta_{ij}|$ . The regularization parameter  $\lambda_{ij}$  for each connection’s coefficient<sup>2</sup> is found through Bayesian optimization embedded in the LOO CV (see Yang et al. (2024)).
3. **Edge-wise fitting with Ridge:** The same as the second setting, but  $p(\theta_{ij}) = \lambda_{ij} \sum_{i,j} \theta_{ij}^2$  the L2-regularization.

<sup>1</sup>Negative values in the functional connectivity matrices indicate an ‘inhibitory’ connection, where increased activity in one cortical region is correlated with a decrease in the other region.

<sup>2</sup>Not to be confused with the shrinkage parameter *lambda*, whereby in this work we distinguish them by using the Greek letter for the former, and English word for the latter.

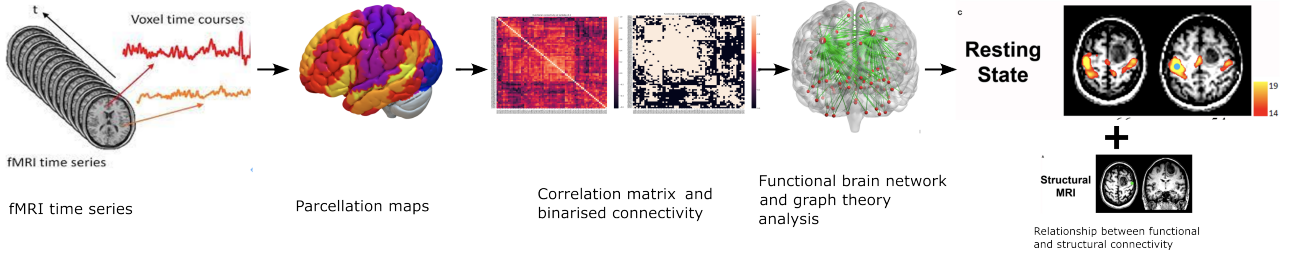


Figure 3. The main workflow from raw functional and structural MRI data to insights gained from graph metrics and linear models.

4. **Single-set coefficient:** we ignore there are connections for each pairwise cortical region, and fit one coefficient for all regions. This is done by flattening both  $S$  and  $\mathcal{F}$  to a vector of size  $19*68*68$ . As a result, per model, there is more data available for fitting compared to the above experiment settings.
5. **Single-set coefficient for each patient:** where we do the same as the fourth setting, but fitting the model each subject. Here, we test for *generalization* by using the fitted parameters for  $N = 1$  patient and evaluate on the remaining  $N = 18$  patients, whereas the model fitting for a patient that achieves a comparatively low error is interpreted to have high generalizability because it predicts accurately on unseen data.
6. **Functional connection density:** We estimate the structural and functional connectivity density for each cortical region by summing across rows of each connectivity matrix, and fit them as in the first setting.

We note that only experiment settings 1 to 3 have AIC/BIC metrics comparable to one another as models are trained with the same data. AIC/BIC metrics from experiments 4, 5 and 6 are better discussed within their setting, not across. Figure 3 summarizes the workflow from the raw MRI data, to obtaining connectivity matrices, and analyzing them through undirected graphs and linear models.

### 3. Experiments and Discussion

#### 3.1. Structural and functional graph metrics are insightful but theory-laden

Graph metrics are sensitive to the thresholds we choose. Figures 4 and 5 illustrate how thresholding affect the spatial distribution of voxels in dMRI and rs-MRI, generally resulting in sparser graphs that can be abstracted. This is because the threshold represents our standard for what is considered a valid/significant connection, where higher values indicate stricter standards<sup>3</sup>. Conversely, higher thresholds can potentially highlight the most robust and significant pathways.

<sup>3</sup>An alternative way to view thresholding is to ignore it and treat each plot as belonging to a different patient, thus thresholding help us observe graphs belonging to 'abnormal' patients compared to a 'healthy' baseline with no thresholding

Figure 4's graph shows that the MSP increases as more voxels are excluded yielding a longer path length between any pair of regions, on average. We observe a slight decrease from 0.7 to 0.8 either because some nodes with large distances have been discarded, or even if there is a large path between remaining nodes, there are so little nodes remaining so that by averaging, the MSP decreases. A similar pattern is reflected in the functional connectome, except there is no dip at higher  $\lambda$  values. Lower MSP values generally indicate a more efficient network with shorter paths between regions, suggesting a highly integrated brain structure conducive to efficient information transfer.

On the other hand, GE continuously decreases in both structural and functional graphs since it is inversely proportional to the MSP. Changes in GE with different FA thresholds can indicate how structural connectivity contributes to the brain's functional integration and segregation. Higher GE suggests a more optimally wired network, which is observed when the brain connectome's integrity is preserved at lower threshold values.

Similarly, both ED and MCC decrease when the threshold increases, and this is related to stringent criteria yielding sparser graphs. Higher ED and MCC indicate integrated brain regions, which could refer to regions of specialized functions. In the FA map, there are 2 spikes that can be noticed on the MCC as threshold increase. In the functional MRI, we also observe an increase in MCC from 0.7 to 0.8  $\lambda$  thresholds. We argue that this pattern occurs for a similar reason as with the MSP: the remaining nodes coincidentally form hubs which on average leads to higher MCC. We wouldn't necessarily see this MCC trend with another patient's brain connectome.

We recall that the functional connectivity matrix has negative correlations. Taking the absolute value slightly changes the values for each graph metric, but doesn't affect the overall trend (Figure 6).

There is no 'correct' threshold to choose in either the dMRI or the rs-MRI. The sensitivity of graph metrics to thresholding is further exacerbated by how we are only working with a single patient's connectome, thus the above results are open to a plethora of interpretations. Such metrics, are, nonetheless, insightful, especially if we have multiple patients to compare with.

Equation	Justification
$f_{ij} = a_{ij} + \beta_{ij}s_{ij}$	Baseline predicting functional connectome directly from structural connectome
$f_{ij} = a_{ij} + \beta_{ij}s_{ij} + \gamma_{ij}t_{ij}^2$	Baseline assuming that the relationship between structural and functional connectivity is not strictly linear.
$f_{ij} = a_{ij} + \beta_{ij}t_{ij}$	Baseline only accounting indirect connections
$f_{ij} = a_{ij} + \beta_{ij}s_{ij} + \gamma_{ij}t_{ij}^2$	Baseline assuming indirect structural and functional connectivity is not linear. Squaring $t_{ij}$ assumes that indirect connections explains more the variance in functional connectome
$f_{ij} = a_{ij} + \beta_{ij}s_{ij} + \gamma_{ij}\sqrt{s_{ij}}$	Baseline accounting for indirect connections
$f_{ij} = a_{ij} + \beta_{ij}\sqrt{s_{ij}}$	Similar as above, where $\sqrt{s_{ij}}$ reflects the diminishing influence of the structural connectivity up to a point where it saturates at higher levels of connectivity
$f_{ij} = a_{ij} + \beta_{ij}s_{ij}^2 + \gamma_{ij}\sqrt{t_{ij}}$	Baseline combining assumptions mentioned above
$f_{ij} = a_{ij} + \beta_{ij}s_{ij} + \gamma_{ij}t_{ij} + \delta_{ij}(s_{ij} \cdot t_{ij})$	The fifth model accounting for the interaction between direct and indirect connections for predicting functional connectivity

Table 1. Candidates linear models and corresponding justification for modelling the functional connectome.  $f_{ij}$  are the pairwise, voxel correlation values between cortical regions  $i$  and  $j$  computed from rs-MRI, and  $s_{ij}$  computed from dMRI.  $t_{ij}$  are indirect structural connections computed following 1. The remaining variables are the corresponding models' parameters.

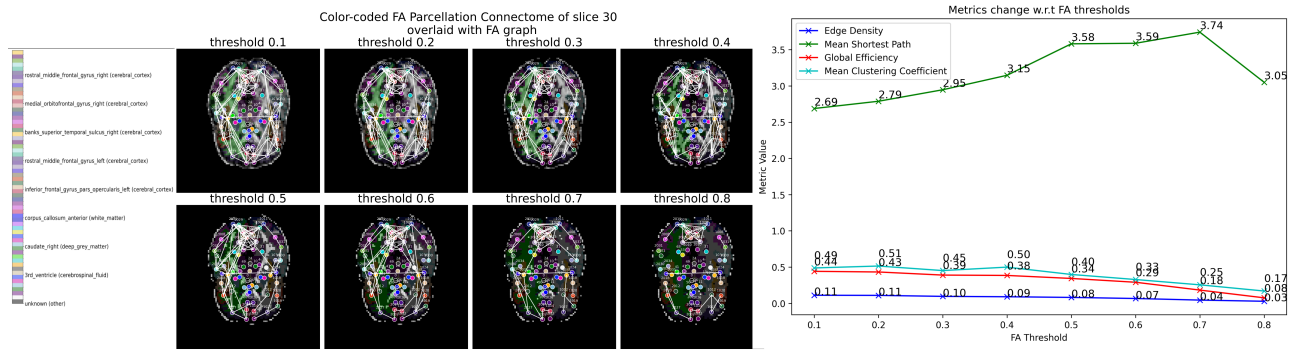


Figure 4. Visualisation of undirected graphs overlaid on FA maps with color-coded, parcelated brain regions across thresholds. On the right we observe how graph metrics vary along thresholds.

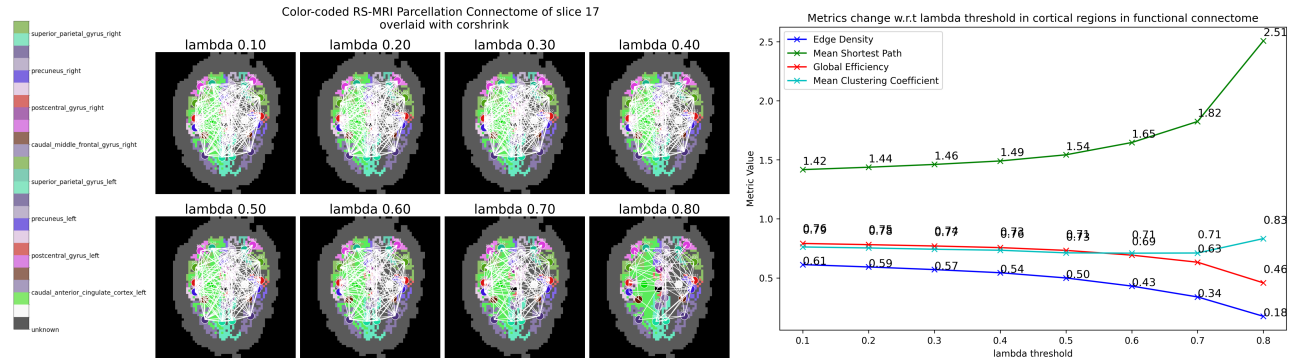
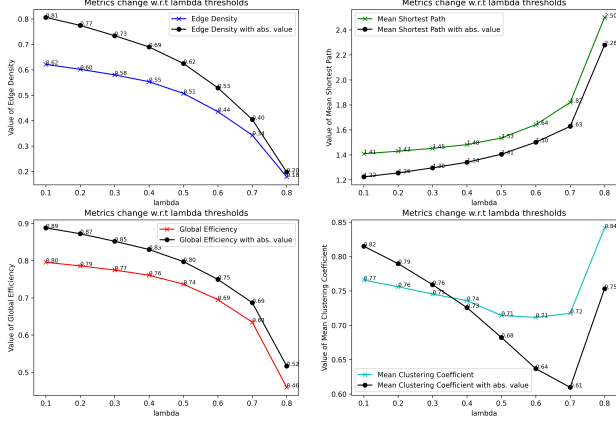


Figure 5. Same visualization as in Figure 4 using rs-MRI data. On the right we observe the pattern of the metrics as the shrinkage parameter varies.

### 3.2. Penalty terms help prevent overfitting

Fitting a standard LR for predicting functional connections lead to overfit coefficients that sometimes yield extremely large MSE values for complex models. In particular, for models 2, 4 which have quadratic terms and 8 which accounts for the interaction between a direct and indirect connection, we observe abnormal MSE values in the order of  $10^5$  since estimated coefficients are also high (see Figure 7 for resulting, abnormal BIC values). We argue this is because these are relatively complex models compared to the baseline, which are known to overfit to small datasets (Cawley & Nicola, 2010), i.e., only  $68^2$  datapoints for 19 patients. We address this by experimenting with both Lasso and Ridge. For the former, Bayesian optimization finds  $\lambda = 0.066$  to be the optimal regularization for

each model variant in each region. Lasso regression manages to converge to a minimum, average MSE across all regions of 0.0032. This is most likely because to avoid multicollinearity and overfitting, it turns coefficients of complex models to zero, thus nested complicated models simplify to the baseline's functional form (see how predictions for all Lasso models are similar in Figure 9). The model of best fit in terms of AIC/BIC/MSE metrics in the 3 experimental settings is the baseline, which we explain with the same reason as above: this is a small dataset, with low number of cortical regions, for a single patient. As such, a simplified model that matches the complexity of the data fits the better. Complicated models would have their coefficients set close to 0 by Lasso, thus even if MSE values converge for all Lasso models, average AIC/BIC would break the tie by accounting for number of parameters (see Figure 8 for



**Figure 6.** Patterns in graph metrics w.r.t  $\lambda$  thresholds before and after taking absolute value of the functional connectivity matrix, discarding negative correlations

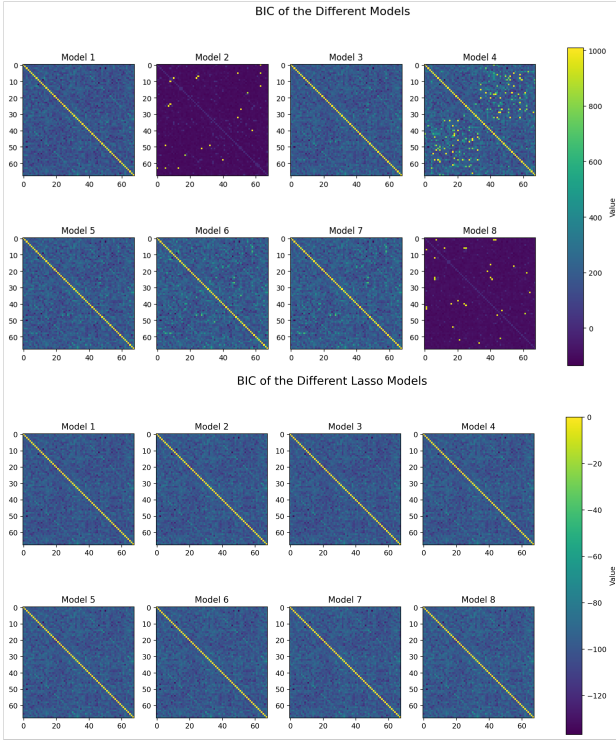


**Figure 7.** Heatmaps of pairwise BIC values representing model fit for each connection. The top panel corresponds to LR models, were models 2, 4 and 8 show yellow dots corresponding to abnormal values which are mitigated using Lasso regression, as shown by the absence of abnormal values in the panel below.

cross-modal comparisons of average AIC/BIC values for all regions). For more detailed results across experimental settings, see Table 2.

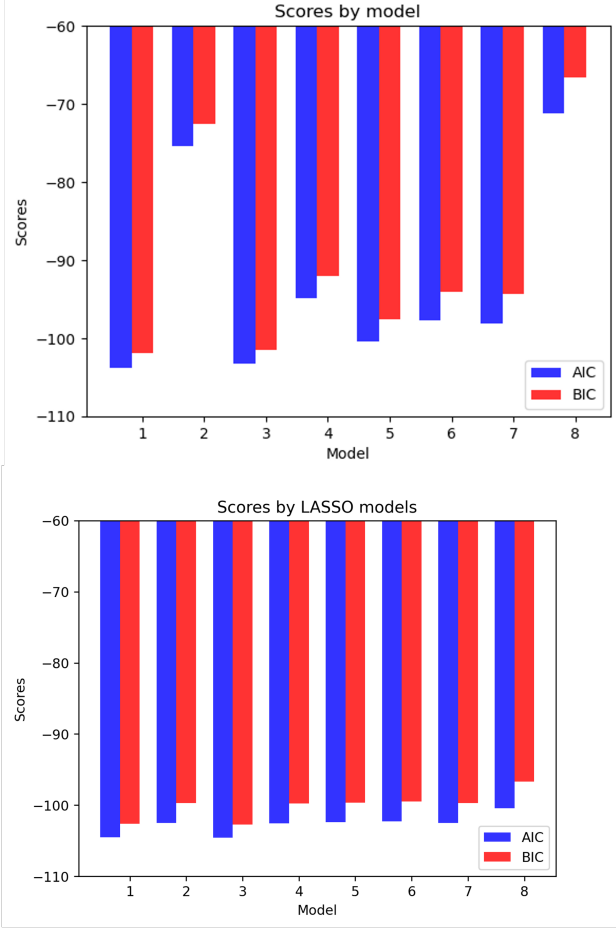


**Figure 8.** Bar graph comparing average of AIC/BIC values across all fit connections. Top panel corresponds to standard LR models, ignoring abnormal AIC/BIC values, while bottom panel corresponds to Lasso variants.

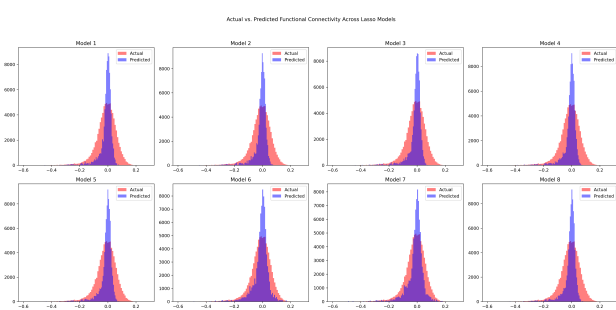


**Figure 9.** Histograms illustrating predicted vs. actual functional connection values, where we note all Lasso models predict in a similar way

### 3.3. Single-coefficient and patient-wise fitting don't perform well

Within the fourth experiment setting, we find model 4 to be the best single-set coefficient architecture. As such, we can interpret this as when we ignore cortical regions by not fitting for each connection, then an expressive model

that accounts for direct and indirect connections performs better. Its best MSE is 0.0173, which is orders of magnitude greater than MSE values obtained from fitting for each connection. This underscores the importance of accounting the complexity and relationship of the different cortical regions.

Fitting for each patient also yields model 4 the best, achieving the lowest MSE when predicting for the remaining 18 patients when fit on patient 14. For all patients, MSE values hover around [0.018, 0.019], which is worse than above in addition to being magnitudes higher than experiment settings 1 to 3. We thus interpret these results as the model not generalizing well, most likely because fitting on a single patient while ignoring the relationship between cortical regions is not enough to learn to predict well on unseen connectivity.

### 3.4. Connection density fitting leads to weak association between modalities

We find model 1, the baseline, to be the best performing in this experiment setting. However, its MSE value is 0.066, which is higher than all prior experiments settings, which we interpret as it is challenging to predict functional connection density from the structural, indicating a weak association between them. This could be explained by how summing out rows in the connectivity matrix leads to information loss of the pairwise cortical connections, and as such the corresponding density vector loses the semantic information that could be previously captured by our proposed models in settings 1 to 3.

### 3.5. Limitations

There is a spectrum of experimental settings we haven't tried, such as fitting a model for each functional edge, for each patient and observe generalizability. Our current data is also small, which leads to several issues we reported in this work such as overfitting. In future work, we can address these limitations by collecting a larger dataset for multiple patients, which is particularly interesting for comparing healthy and abnormal connectomes for clinical purposes, as well as performing more comprehensive experiments to understand how functional connectivity is related to the structural. With larger datasets, however, we would require more complicated, non-linear models to capture the complicated relationship between functional and structural connections, relaxing implicit assumptions such as that all edges share a similar relationship as in experimental settings 1 to 3, or accounting for only one-hop indirect connections.

## 4. Conclusions

Connectomics is a rapidly advancing field thanks to the wealth of data made available thanks for powerful non-invasive, brain imaging techniques, along with ML analysing tools.

Experiment setting	Best model index	best avg. AIC	best avg. BIC	best avg. RMSE
Edge-wise LR	1	-105.83	-101.97	0.0034
Edge-wise LR + Lasso	1 and 3	-104.69	-102.83	0.0032
Edge-wise LR + Ridge	3	-104.58	-102.78	0.0032
singe-set coefficient LR	4	-356279.22	-356260.45	0.017
single-set coefficient LR for each patient	4 for patient 14	-19376.63	-19363.75	0.015
LR for functional connection density	1	-49.68	-47.90	0.066

*Table 2.* Results for the different experimental settings, each setting ran with leave one out cross-validation. Comparisons can only be made within an experimental setting. Across experimental settings, with the exception of the first, second and third, we notice that different data points are used, and as such AIC, BIC and MSE which depend on the log-likelihood can't be compared. LR stands for linear regression.

On one hand, we observe how graph theory can be insightful for understanding the brain's structural and functional connectome, but nonetheless challenging. Although graph representations are a convenient way to visualise the underlying data, the graph is implicitly subject to all of the caveats in the process of generating it, such as no principled way to 'threshold' what constitutes a node. As we showed, the arbitrarily chosen thresholds affect the appearance of the graph with density of clusters and connectivity changing.

In terms of fitting linear models, we showed that functional connectivity is found between regions that are both anatomically connected but also disconnected, which reproduces the current paradigm in literature. For future work, it would be interesting to explore how robust network effects are across different patient populations both in healthy and pathological context, as well as comparing the differences between patient subpopulations such as controlling for age or sex.

---

## References

- Cawley, Gavin C and Nicola. On over-fitting in model selection and subsequent selection bias in performance evaluation. *The Journal of Machine Learning Research*, 11:2079–2107, 03 2010. doi: 10.5555/1756006.1859921.
- Deligianni, Fani, Varoquaux, Gael, Thirion, Bertrand, Sharp, David J, Ledig, Christian, Leech, Robert, and Rueckert, Daniel. A framework for inter-subject prediction of functional connectivity from structural networks. *IEEE Transactions on Medical Imaging*, 32:2200–2214, 12 2013. doi: 10.1109/tmi.2013.2276916.
- Farahani, Farzad V., Karwowski, Waldemar, and Lighthall, Nichole R. Application of graph theory for identifying connectivity patterns in human brain networks: A systematic review. *Frontiers in Neuroscience*, 13, 06 2019. doi: 10.3389/fnins.2019.00585.
- Pavlopoulos, Georgios A, Secrier, Maria, Moschopoulos, Charalampos N, Soldatos, Theodoros G, Kossida, Sophia, Aerts, Jan, Schneider, Reinhard, and Bagos, Panagiotis G. Using graph theory to analyze biological networks. *BioData Mining*, 4, 04 2011. doi: 10.1186/1756-0381-4-10.
- Rubinov, Mikail and Sporns, Olaf. Complex network measures of brain connectivity: Uses and interpretations. *NeuroImage*, 52:1059–1069, 09 2010. doi: 10.1016/j.neuroimage.2009.10.003.
- Schäfer, Juliane and Strimmer, Korbinian. A shrinkage approach to large-scale covariance matrix estimation and implications for functional genomics. *Statistical Applications in Genetics and Molecular Biology*, 4, 01 2005. doi: 10.2202/1544-6115.1175.
- Wu, Chengyuan, Ferreira, Francisca, Fox, Michael, Harel, Noam, Hattangadi-Gluth, Jona, Horn, Andreas, Jbabdi, Saad, Kahan, Joshua, Oswal, Ashwini, Sheth, Sameer A., Tie, Yanmei, Vakharia, Vejay, Zrinzo, Ludvic, and Akram, Harith. Clinical applications of magnetic resonance imaging based functional and structural connectivity. *NeuroImage*, 244:118649, 12 2021. doi: 10.1016/j.neuroimage.2021.118649. URL <https://www.sciencedirect.com/science/article/pii/S1053811921009228>.
- Yang, Kaixin, Liu, Long, and Wen, Yalu. The impact of bayesian optimization on feature selection. *Scientific Reports*, 14:3948, 02 2024. doi: 10.1038/s41598-024-54515-w. URL <https://www.nature.com/articles/s41598-024-54515-w>.

---

## 5. Appendix

**Algorithm 1** General algorithm for obtaining indirect paths between cortical regions  $i$  and  $j$  from structural correlation matrix computed from dMRI

---

```
1: Initialize indirect_connections
2: for each subject: do
3:   for each pair of cortical regions i and j: do
4:     exclude the same region
5:     Initialize min_weights array to store minimum weights
6:     for For each intermediate region k (loop over cortical regions): do
7:       If k is neither regions i or j:
8:         min_weight = min(structural_matrixes[subject_index, i, k], structural_matrixes[subject_index, k, j]) #Calculate the minimum weight between regions i and k, and between regions k and j.
9:         Append min_weight to min_weights
10:        If min_weights isn't empty:
11:          Append max(min_weights) to indirect_connections[subject, i, j] #This represents the maximum of all minimum weights along different paths from region i to region j through intermediate regions k.
12:      end for
13:    end for
14:  end for
```

---